



Seismic response of RC frames with HSTC beams endowed with friction damper devices

Salvatore Pagnotta^a, Piero Colajanni^a, Lidia La Mendola^a, Alessia Monaco^b

^a Department of Engineering, Viale delle Scienze, Ed. 8, 90128 Palermo, Italy

^b Department of Architecture and Design, Politecnico di Torino, Viale Mattioli 39 - 10125 Torino, Italy

Keywords: friction dampers; hybrid steel-trussed-concrete beams; cyclic behaviour of beam-column joints

ABSTRACT

The aim of this work is to compare the seismic response of RC frames built using Hybrid Steel-Trussed Concrete Beams (HSTCBs) whether or not equipped with friction damper devices installed at the beam-to-column joints. Due to their small depth-to-span ratios, HSTCBs usually lead to a large amount of rebar within the beam-column joint, potentially reducing its cyclic performance. Therefore, the adoption of a friction system at the beam-to-column joint provides two main advantages, i.e. limiting the shear forces, and thus the potential damage, in the panel zone thanks to the increasing of the bending moment lever arm, and assigning to the device the task of dissipating the incoming seismic energy, thus preventing damage to the end sections of the beams. The seismic response of traditional and innovative r.c. frames is computed by means of non-linear time history analysis, taking into account the degrading phenomena, both in terms of stiffness and strength, which are observed in beam-column joints when subjected to cyclic actions. The cyclic behaviour of the beam-column joint of the traditional frame is tuned on the results of cyclic test on a full scale beam-column joint subassembly. The results highlight that RC frame endowed with friction devices provide structural performance consistent with design forecasts, i.e. beam end sections with a nearly-elastic behaviour, panel zones which experience negligible level of damage, comparable values of both maximum interstorey drift ratio and amount of energy dissipated with respect to traditional frame.

1 INTRODUCTION

Over the last decades, a new design philosophy is gaining popularity in earthquake-prone areas, based on the use of energy dissipating devices (e.g.: friction, metallic, viscoelastic, viscous) able to absorb the seismic energy preserving the structural members from damage. This approach answers to the need expressed by stakeholders to have buildings which experience low or no damage during main shocks, and subsequent aftershocks, in order to be operative as soon as possible after the seismic events. As a matter of fact, traditional Moment Resisting Frames (MRFs) are based on a “high damage” concept, namely the seismic energy is absorbed by plastic hinges at beam ends, leading to potentially highly damaged structural members after a strong earthquake. Unfortunately, the cost of repairing the structural (and non-structural) damage cumulated is often higher than the cost of

reconstruction. Furthermore, the cost related to the non-operability of the building has to be considered as well. In light of this, traditional MRFs are not environmentally and economically sustainable. In this context, regarding energy dissipating devices based on friction, several studies have been carried out in order to develop devices able to dissipate the seismic energy (Borzouie et al. 2016; Ramhormozian et al. 2018; Zimbru et al. 2018; Latour et al. 2019). The main goal of these devices is to dissipate the seismic energy exploiting friction forces generated through plates made with several materials (e.g.: coated steel, polymeric, composite) and clamped together by means of preloaded bolts. Thus, the traditional structural members surrounding the friction device are prevented by damage, remaining in a nearly-elastic behaviour. Several friction device configurations have been developed for steel structures (e.g.: Yang & Popov 1995; Butterworth & Clifton 2000; Khoo et al. 2015; Latour et al. 2015; Latour et al. 2018), while few studies concern friction devices

employed in RC structures (e.g.: Morgen & Kurama 2004; Tsampras et al. 2018). The aim of this work is to compare the seismic response of RC frames built using HSTCBs whether or not equipped with friction damper devices installed at the beam-to-column joints. HSTCBs represent a structural solution that has been widely exploited by the construction industry over the last thirty years due to the several advantages related to the partial industrialization of the construction process of framed structures. The analysed HSTCB (Colajanni et al. 2015, 2018a, 2018b) is constituted by a spatial steel lattice built using inclined V-shaped rebars. These rebars, which represent the transverse reinforcement of the beam, are also joined at the top to a variable number of bars constituting the upper chord by means of fillet welds, while at the bottom to a plate usually employed in constructional steelwork. The above-described truss is made up in factory and then the beam is completed with cast-in-situ concrete.

Thanks to a reinforcement formed by a steel truss, HSTCBs are able to cover long spans with small section depths. This characteristic requires the use of large amount of reinforcement in the beam-to-column joints, often employing large diameter bars. Thus, both the beam ends and the joint panel become vulnerable to the effects of cyclic actions, like those induced by seismic excitation. Even if at beam ends the presence of a properly-designed transverse reinforcement, which provides confinement to the concrete, is usually able to reduce the loss of both stiffness and strength due to cyclic actions, large diameter bars inside a small-sized joint panel cause concrete cracking and damage, inducing a loss of bond. This phenomenon causes degrading hysteresis cycles, which may bring to a reduced structural dissipative capacity.

The use of dissipative devices, entrusting them with the task of dissipating energy, prevents damage to the structural elements, improving the expected performance, drastically reducing the economic losses due to the structural repair in the event of violent earthquakes. Moreover, using suitably-designed devices, characterized by increased lever arm of the bending moment transferred from beams to the joint, it is possible to reduce the shear forces acting on the joint panel, preventing its damage. With the aim of keeping the RC elements in an almost elastic field, according to capacity design criteria, they have to be properly overstrengthened. This target is hampered by the uncertainties affecting friction devices due to the variability in the application of bolt preload and to the value of the friction

coefficient of surfaces involved in the sliding.

In the proposed work, the seismic response of RC frames is calculated through non-linear time history analysis (NLTHA), using models able to represent the cyclic behaviour of both joint panel and friction dissipating device. The analysed frame models take into account the degrading phenomena, both in terms of stiffness and strength, which are observed in beam-column joints when subjected to cyclic actions, by means of link elements, whose cyclic behaviour is calibrated using the results of experimental tests. NLTHA results, confirm the design forecasts, namely the energy dissipated by plastic hinges in the traditional frame is absorbed by friction devices in the innovative one. By doing so, beam end sections remain within the elastic range, proving the superior performances of the systems equipped with friction devices, both in energy dissipation capacity and damage prevention.

2 MACRO MODELLING OF THE CYCLIC BEHAVIOUR OF RC BEAM-COLUMN JOINTS

The first step to carry out the comparison between RC frames endowed or not with friction devices is to properly model the cyclic behaviour of RC beam-column joints. As a matter of fact (Pan et al., 2017), beam-column joints undergo significant shear deformations, often exhibiting stiffness and strength deterioration, which greatly contribute to storey drifts during earthquake loading. For this reason, in order to model the cyclic behaviour of beam-to-column joint of traditional RC frames made with HSTCBs, the results of a previously-carried out experimental campaign are used, reported in (Colajanni et al. 2016). The subassemblies tested were representative of four-way nodes, constituted by two half-columns having cross-section dimensions equal to 300x400 mm, reinforced with 10 rebars of 20 mm diameter, while the beams are made with a truss having a lower steel plate 5 mm thick, three coupled bars 16 mm diameter which constitute the upper chord of the truss and diagonal web bars 12 mm diameter placed at a 300 mm spacing. The cross-section of the beam is 300 mm width and 250 mm depth. In the section of the beam next to the column it has to be taken into account the resistance contribution of the added reinforcing rebars only, neglecting the contribution of the truss. Therefore, the upper and lower areas of the reinforcement in the sections next to the joint are equal to 1808 mm² and 904 mm² each, which are

due to 4Φ24 and 2Φ24 respectively. The scheme of the constraints and load condition of the specimens is reported in Figure 1.

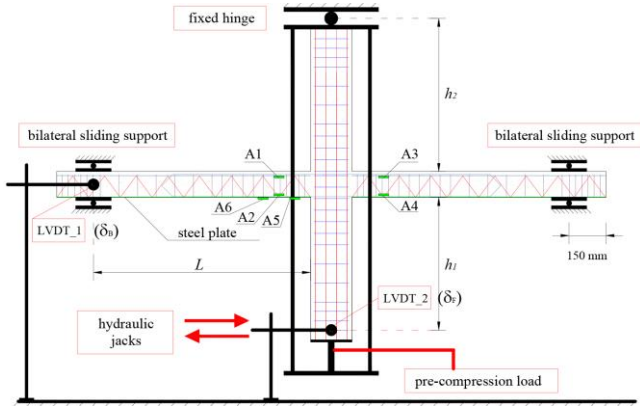


Figure 1. Scheme of the constraints and load condition of the specimens (from Colajanni et al. 2016)

The results have shown a degrading behaviour in terms of strength, stiffness and pinching of hysteretic cycles. Among the three subassemblies tested, specimen N. 2 is selected in order to calibrate the cyclic behaviour of the joint. With the aim of taking into account the above-mentioned degrading phenomena in the analysis of RC frames, the model proposed by Lowes & Altoontash (2003) is adopted. This model, represented in Figure 2, is constituted by a four-node, 12 DOFs super-element which comprises:

- A shear-panel component that simulates strength and stiffness loss due to failure of the joint core;
- Eight bar-slip springs that simulate stiffness and strength loss due to anchorage-zone damage;
- Four interface-shear springs that simulate reduced capacity for shear transfer at the joint perimeter due to crack opening.

This model employs the Modified Compression Field Theory (MCFT) (Vecchio & Collins 1986) to define the envelope to the shear stress versus strain history of the joint core. As shown in Figure 2, the joint model is developed assuming that all joint loads, including column axial load, are transferred through shear loading of the joint core. Thus, in applying the MCFT, normal stresses are defined to be zero and normal strains are assumed to be negligible. In the model proposed by Lowes & Altoontash, the cyclic response of joint core is calibrated using experimental study carried out by Stevens et al. (1991). In the present paper, with the aim of simplifying the study, parameters proposed by Sivaselvan & Reinhorn (2000) are employed, as will be discussed later.

The envelope to the bar-stress versus –slip relationship is developed on the basis of several

simplifying assumptions about joint anchorage-zone response. First, bond stress along the anchored length of a reinforcing bar is assumed to be uniform for reinforcement that remains elastic or piecewise uniform for reinforcement loaded beyond yield. Second, slip is assumed to define the relative movement of the reinforcing bar with respect to the perimeter of the joint and is a function of the strain distribution along the bar. Third, the bar is assumed to exhibit zero slip at the point of zero-bar stress. Figure 3 shows an idealization of the bond stress and the resulting bar-stress distribution for an anchored bar loaded beyond yield. Parameters identified in Figure 2 are defined in the following section.

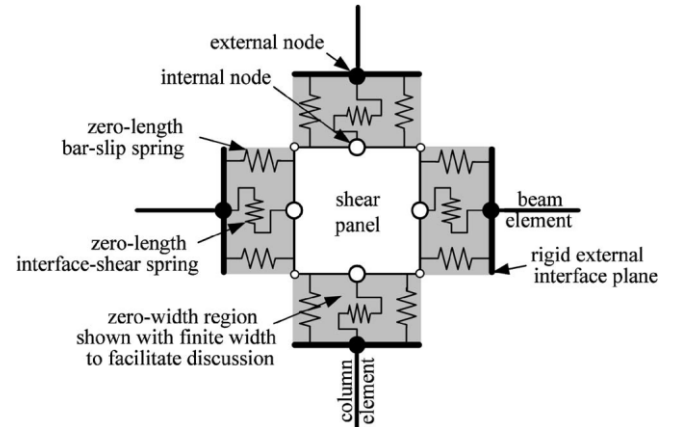


Figure 2. RC beam-column joint model (from Lowes & Altoontash 2003)

Once these simplifying assumptions have been employed, the bar-stress versus –slip relationship is defined as follows:

$$s = 2 \frac{\tau_{ET} l_{fs}^2}{E d_b} \quad f_s \leq f_y \quad (1)$$

$$s = 2 \frac{\tau_{ET} l_e^2}{E d_b} + \frac{f_y}{E} l_y + 2 \frac{\tau_{YT} l_y^2}{E_h d_b} \quad f_s > f_y$$

with

$$l_{fs} = \frac{\tilde{f}_s}{\tau_{ET}} \frac{A_b}{\pi d_b} \quad l_e = \frac{f_y}{\tau_{ET}} \frac{A_b}{\pi d_b} \quad (2)$$

$$l_y = \frac{\tilde{f}_s - f_y}{\tau_{YT}} \frac{A_b}{\pi d_b}$$

where:

- \tilde{f}_s : bar stress at the joint perimeter;
- f_y : the steel yield strength;
- E : steel elastic modulus;
- E_h : steel hardening modulus assuming a bilinear stress-strain response;
- τ_{ET} : bond strength for elastic steel;

τ_{YT} : bond strength for yielded steel;

A_b nominal bar area;

d_b nominal bar diameter.

Moreover, l_e and l_y , define, respectively the lengths along the reinforcing bar for which steel stress is less than and greater than the yield stress. For the case of $l_e + l_y$ greater than the width of the joint, the deterioration of bond strength under cyclic loading will be much more severe. In this case, it may be appropriate to assume reduced bond strength in the elastic region of the reinforcing bar.

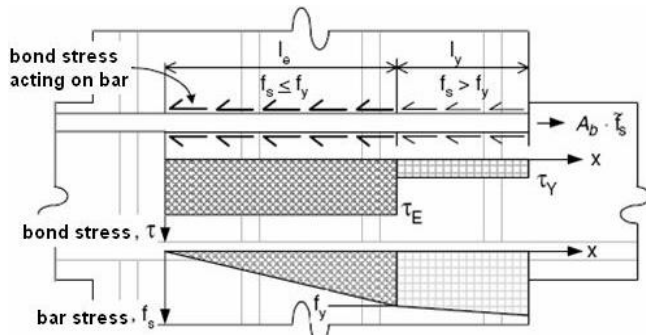


Figure 3. Bond stress and bar stress distribution for a bar anchored in a beam-column joint (from Lowes & Altoontash 2003)

The bar-stress versus -slip relationship defined by Eq. (1) monotonically increases. However experimental data indicate that bond strength deteriorates once a “slip limit” is exceeded (Eligehausen et al., 1983). Here, bond strength is assumed to deteriorate once slip exceeds 3 mm, and post-peak stiffness is defined equal to 10% of the initial stiffness. With respect to the bond strength values to be adopted in Eq. (1), experimental testing of anchorage-zone specimens and structural subassemblies (e.g.: Eligehausen et al., 1983) indicates that bond strength is a function of material state of the anchored bar as well as of the concrete and transverse reinforcing steel in the vicinity of the bar. In this paper, as proposed by Lowes & Altoontash (2003), values of $1.8 f_c^{0.5}$ and $0.2 f_c^{0.5}$ are adopted for τ_{ET} and τ_{YT} , respectively, being f_c the compressive strength of concrete.

Interface-shear springs are considered elastic due to lack of experimental data for use in calibrating these components.

3 ANALYSIS OF THE RC BEAM-COLUMN JOINT AS BENCHMARK TEST

In this section, the macro model described in the previous section is implemented in a structural software with the aim of comparing the analytical and experimental cyclic curves. In this

paper, both benchmark test on the subassembly and NLTHAs on RC frames realized with traditional beam-to-column connections or employing innovative friction damper devices are carried out using the software SeismoStruct (Seismostruct, 2016). Structural members are modelled using distributed plasticity fiber-section elements with force-based formulation, while shear-panel component and bar-slip springs are modelled by means of link element. The latter is a 3D element, having uncoupled axial, shear and flexural behaviours, which links two coincident structural nodes defining a force-displacement or moment-rotation response relationship independent for each of its 6 DOFs. In Figure 4 the structural model employed to adapt the aforementioned beam-column joint model into the software is represented.

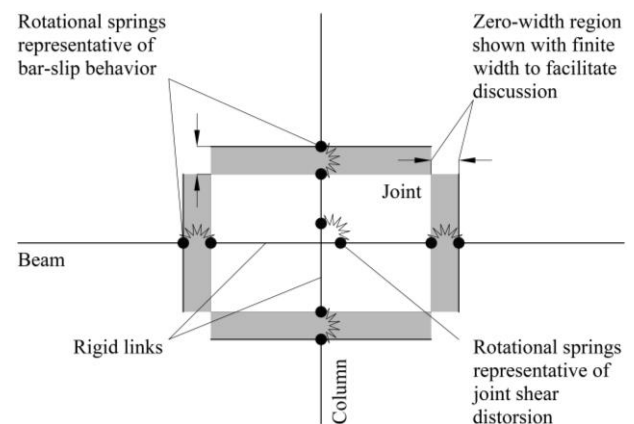


Figure 4. Structural model implemented in SeismoStruct

It is constituted by:

- Four rotational springs at the beam-to-joint and column-to-joint interfaces to model the rotation of the structural member due to the slip of the longitudinal reinforcement through the joint;
- One rotational spring at the centre of the beam-column joint to model the relative rotation between beams and columns due to the shear deformation of the joint region.

Moreover, four rigid links are introduced between central nodes and nodes on the beam-to-joint and column-to-joint interfaces, assuming that the cyclic behaviour of the joint is totally represented by the central rotational spring. These rotational springs are modelled by means of link elements in which a moment-rotation behaviour is defined using the Multilinear (multi-lin) constitutive law. This is the Polygonal Hysteretic Model (PHM) introduced by (Sivaselvan & Reinhorn 1999), which is able to simulate stiffness and strength deterioration and pinching phenomenon. The parameters through which the backbone curve is defined are computed using the

above-described procedures, while those able to model the cyclic behaviour are calibrated using the values proposed by Sivaselvan & Reinhorn (2000) for the joint core. The parameters governing the bar-slip mechanism are tuned on the basis of the experimental results. In Table 1 the parameters defining the “Multilinear” spring elements for the panel zone and the bar-slip mechanism are reported.

Table 1. Parameters of the “Multilinear” spring element adopted for modelling the cyclic behaviour of the Panel Zone (PZ) and the Bar-Slip mechanism (BS)

| First-class parameters (backbone curve) | PZ | BS |
|---|--------|---------|
| Initial rotational stiffness (kNm/rad) | 235000 | 46000 |
| Cracking moment (kNm) | 47 | 90/-166 |
| Yielding moment (kNm) | 290 | 92/-170 |
| Yield rotation (rad) | 0.006 | 0.03 |
| Ultimate rotation (rad) | 0.2 | 0.12 |
| Post-yield stiffness ratio as % of elastic | 0.001 | 0.01 |
| Second-class parameters (hysteresis shape) | PZ | BS |
| Stiffness degradation | 4 | 4 |
| Ductility based strength decay | 0.6 | 1 |
| Hysteretic energy based strength decay | 0.6 | 0.001 |
| Slip parameter | 0.5 | 0.35 |

The comparison between experimental and analytical curves is reported in Figure 5.

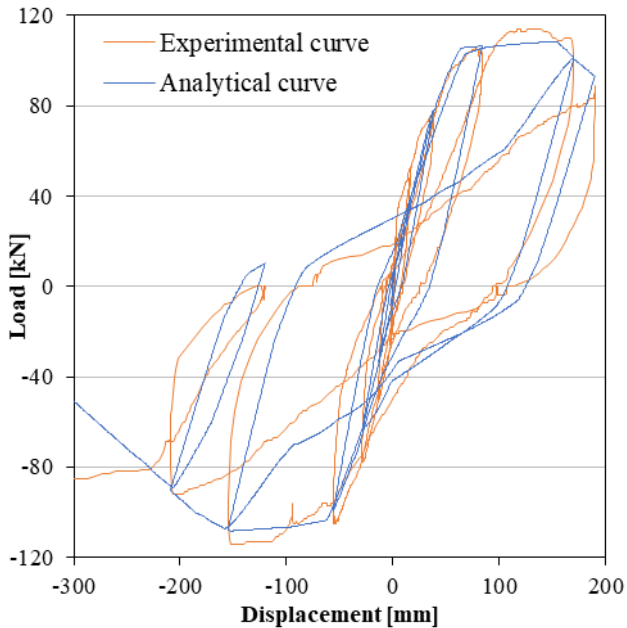


Figure 5. Comparison between experimental and analytical curves

It can be seen that the structural model is able to reproduced stiffness and strength deterioration and pinched hysteretic cycles. Once the cyclic behaviour of the traditional RC beam-column

joint realized with HSTCBs has been modelled, in the next section a brief description of the friction device is reported.

4 DESCRIPTION OF THE FRICTION DEVICE

A thorough analysis of the friction device developed for HSTCBs can be found in (Colajanni et al., 2019). Here, a brief description concerning the configuration of the device is reported. The dissipative connection system between column and HSTCB represented in Figure 6 is constituted by the following components: - the upper T-stub connection anchored to the column and bolted to a “C” steel profile which is welded to the upper longitudinal rebars of the steel truss of the HSTCB; - the friction connection on the bottom, constituted by a vertical central steel plate with curved slotted holes and steel angles anchored to the column; the latter realize the friction connection with the central slotted plate and eventual plies of friction material. These elements are connected by high strength friction bolts properly preloaded according to the slip force required.

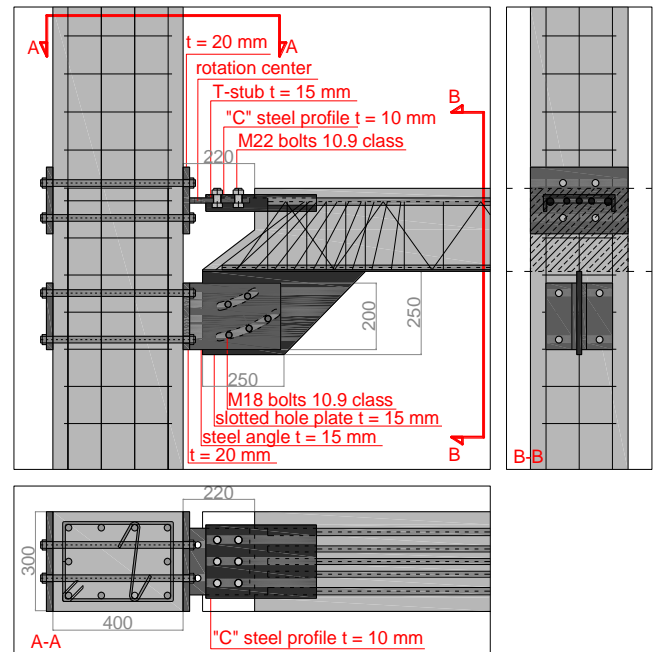


Figure 6. Structural solution adopted for the beam-to-column connection

The design value of the bending moment to activate the slippage of the friction device is set equal to $M_d = 110$ kNm. An overstrength coefficient equal to $\Omega_\mu = 1.5$ is adopted, to take into account the variability of static and dynamic friction coefficients. Thus, the overstrengthed design resisting bending moment is equal to $M_{Rd} = \Omega_\mu M_d = 1.5 \times 110 = 165$ kNm, which is equal to the negative yield moment of the above-

mentioned HSTCB.

As already seen in Colajanni et al. (2019), the cyclic response of the friction device calculated by means of FEM analysis behaves according to the design requirements, i.e. it exhibits a symmetric response for hogging and sagging bending moment and does not evidence any damage in the loading-unloading phases.

5 DEFINITION OF RC FRAME MODELS AND SEISMIC INPUT

In order to perform the comparison between the seismic response of RC frames endowed or not with friction devices, a generic RC frame having two storeys 3 m height and two spans 5 m long is set. Column and beam longitudinal and transverse reinforcements are those of the subassembly described in Section 2. In Figure 7 the structural model of the RC frame investigated is illustrated.

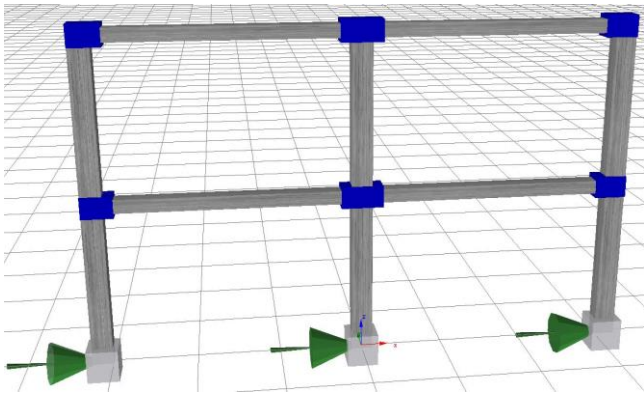


Figure 7. Structural model of the RC frame investigated

On each storey, a distributed mass of 3.8 t/m is added in order to set the fundamental period of the frame, which is equal to 0.5 sec. In Figure 8 the node modelling scheme in case of RC frame with friction device is showed.

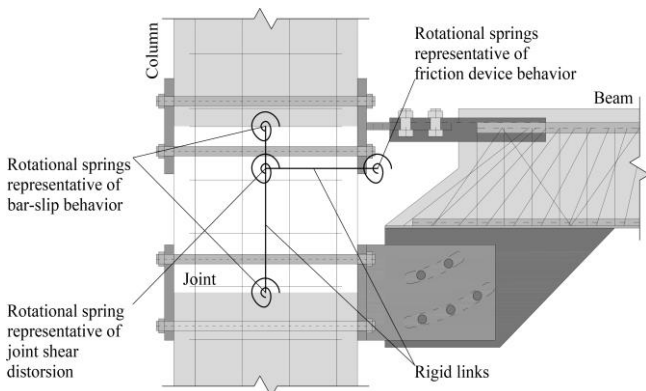


Figure 8. Node modelling scheme in case of RC frame with friction device

The panel zone is modelled as illustrated in Figure 4, with a non-linear rotational spring representative of joint shear deformation, while the friction device is represented by means of a

bilinear kinetic rotational spring. The parameters of the latter are reported in Table 2.

NLTHAs are carried out on the two RC frames with or without friction devices using seven quasi-stationary artificial accelerograms. Each accelerogram has a duration equal to 30 seconds, with a strong motion phase of 20 seconds. In Figure 9 one of these acceleration time history is reported, while in Figure 10 the response spectra and the average one of the seven accelerograms generated are shown.

Table 2. Parameters of the bilinear kinetic rotational spring adopted for modelling the cyclic behaviour of the friction device

| | |
|--|-------|
| Initial rotational stiffness (kNm/rad) | 50000 |
| Yielding moment (kNm) | 110 |
| Post-yield stiffness ratio as % of elastic | 0.01 |

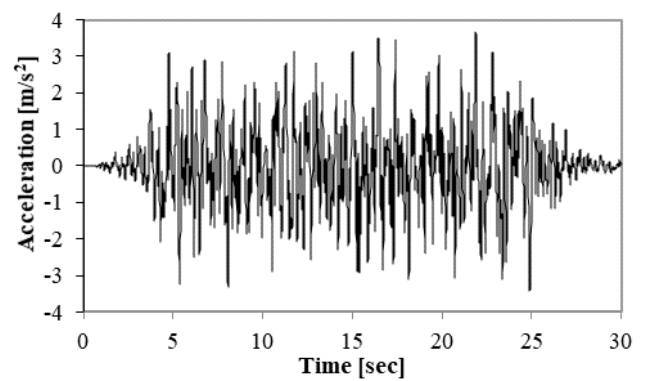


Figure 9. Acceleration time history of one of the seven quasi-stationary accelerograms used

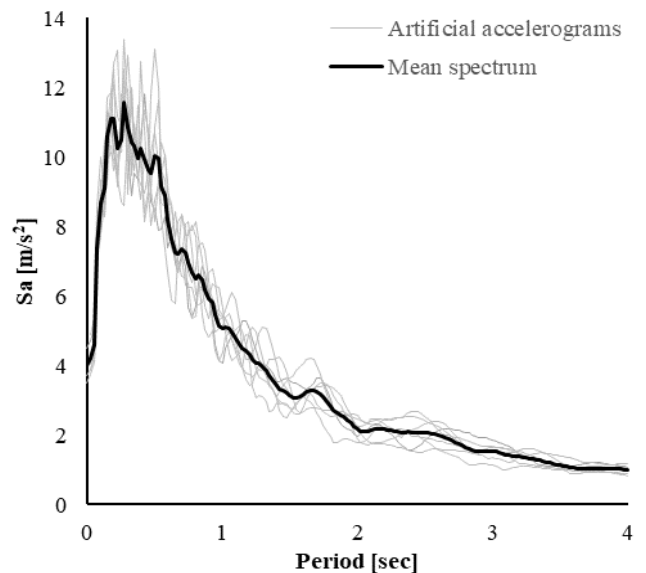


Figure 10. Response spectra and the average one of the seven accelerograms generated

6 ANALYSIS OF RESULTS

Once NLTHAs have been executed, several parameters have been inspected with the aim of understanding the local and global behaviour of

the above-described structures. The structural parameters here investigated are:

- Average and CoV of Maximum Interstorey Drift Ratios (MIDRs);
- Average and CoV of the cumulative amount of energy dissipated;
- Moment-rotation curves of beam end sections;
- Moment-rotation curves of link elements representing panel zone, bar-slip mechanism and friction device.

In Table 3 average and CoV of MIDRs of the two types of RC frames analysed are reported.

Table 3. Average and CoV of maximum interstorey drift ratios of the two types RC frames investigated.

| Storey | | MIDRs of traditional frame | MIDRs of innovative frame |
|--------|---------|----------------------------|---------------------------|
| 1 | Average | 2.82 % | 2.91 % |
| | CoV | 12.51 % | 17.00 % |
| 2 | Average | 2.87 % | 3.06 % |
| | CoV | 13.53 % | 16.85 % |

As can be seen, similar average and CoV values of interstorey drift ratio are provided by traditional and innovative frames, with a slight increment of the values in case of frames endowed with friction devices.

In Figure 11 the average and CoV of the cumulative amount of energy dissipated by the frames, normalized by the average total energy dissipated by traditional frame are illustrated.

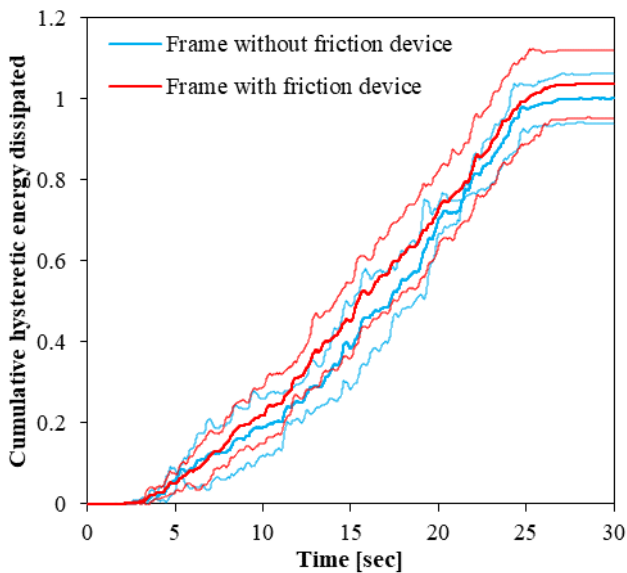


Figure 11. Average and CoV of the cumulative amount of energy dissipated by traditional and innovative frames

As expected, RC frames endowed with friction devices show a similar performance in terms of cumulative hysteretic energy dissipated compared to traditional ones.

For the sake of simplicity, in order to compare the different behaviours of the two different RC frame configurations, only the moment-rotation

curves of the following elements are reported here:

- Right end of the first-storey first-span beam (Figure 12, Figure 13);
- Link element representing the beam-column joint shear distortion of the first-floor internal joint (Figure 14, Figure 15);
- Link element connected to the right end of the aforementioned beam representing the bar-slip mechanism (in case of traditional frame) (Figure 16);
- Link element connected to the right end of the aforementioned beam representing the friction device (in case of innovative frame) (Figure 17).

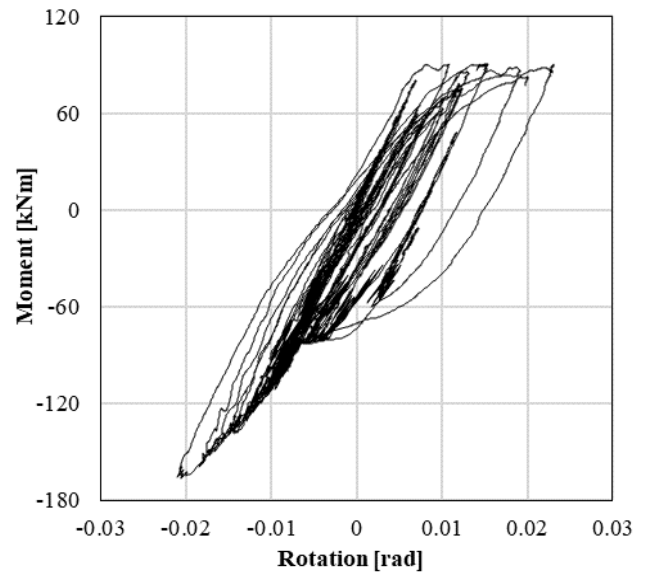


Figure 12. Traditional frame: moment-rotation curve of the investigated beam section

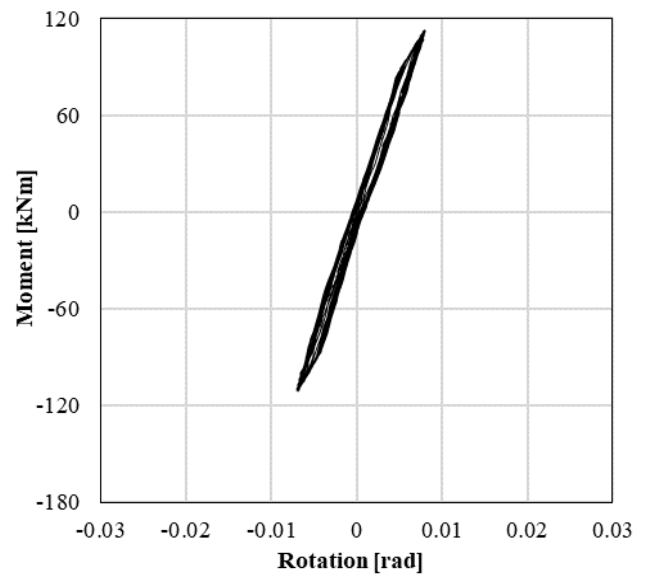


Figure 13. Innovative frame: moment-rotation curve of the investigated beam section

The investigated beam end of the traditional frame (Figure 12) undergoes severe plastic deformations due to the yielding of the bottom longitudinal bars. On the contrary, consistently

with design provisions, the investigated beam end of the innovative frame (Figure 13) shows a nearly-elastic moment-rotation curve.

With reference to the link elements representing the cyclic behaviour of the beam-column joint investigated, it can be seen that the panel zone of the traditional frame (Figure 14) experiences loss of strength and stiffness, achieving a significant level of damage. By contrast, the panel zone of the innovative frame (Figure 15) does not reach the yield moment, thus the degrading phenomena in terms of strength and stiffness are not activated. Therefore, the damage undergone by the panel zone is negligible, being limited to crack formation.

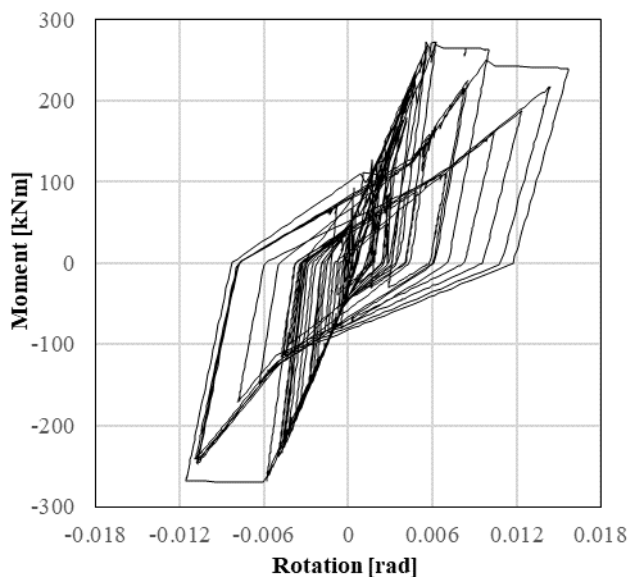


Figure 14. Traditional frame: moment-rotation curve of the link element representing the beam-column joint shear deformation of the first-floor internal joint

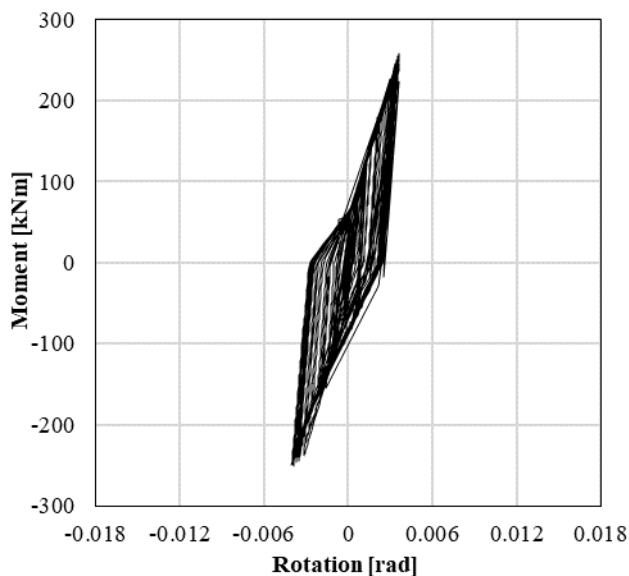


Figure 15. Innovative frame: moment-rotation curve of the link element representing the beam-column joint shear deformation of the first-floor internal joint

In the traditional frame, link element representing the bar-slip phenomenon (Figure 16)

shows a degrading cyclic performance as well, contributing to the global level of damage experienced by the beam-column joint in the traditional frame.

Lastly, with respect to the link element representing the friction device (Figure 17), it can be noticed that the seismic energy previously absorbed by plastic hinges of beams is dissipated, in the innovative frame, by friction device. The hysteretic cycles of the friction damper are wide and stable, having assumed that cyclic performance of the device are not dependent on cumulative displacement experienced.

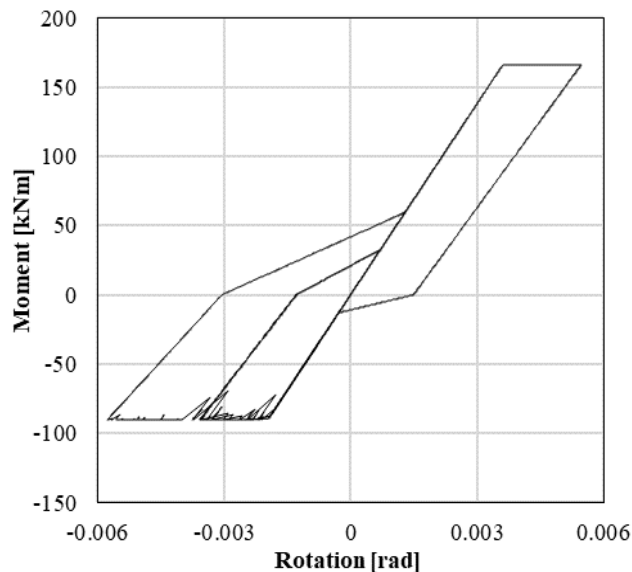


Figure 16. Traditional frame: moment-rotation curve of the link element connected to the investigated beam section representing the bar-slip mechanism

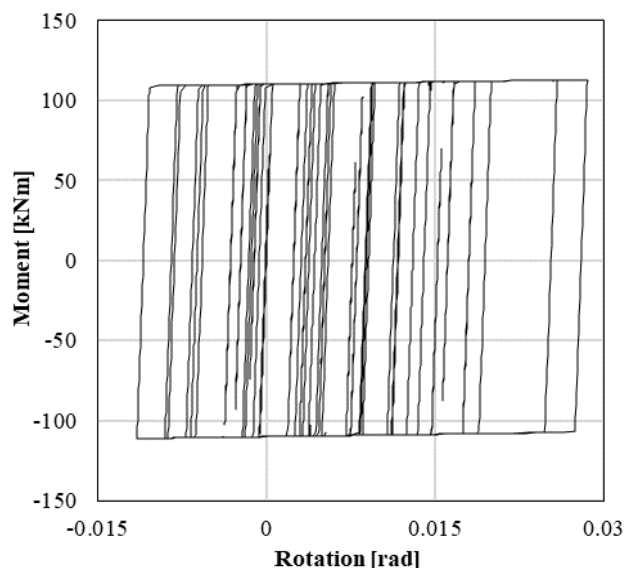


Figure 17. Innovative frame: moment-rotation curve of the link element connected to the investigated beam section representing the friction device

7 CONCLUSIONS

In this paper, a comparison between RC frames realized with HSTCBs endowed or not with friction devices has been carried out. The degrading phenomena affecting the cyclic performance of the beam-column connections (i.e.: joint shear distortion and slippage of the longitudinal bars within the panel zone) have been taken into account by means of the macro model proposed by Lowes & Altoontash (2003). The cyclic behaviour of the macro model has been modelled on the basis of a previously-carried out experimental tests on beam-column subassemblies realized by means of HSTCBs. The seismic response of the traditional and innovative frames has been evaluated via NLTHAs, using quasi-stationary artificial accelerograms. As expected, the results highlight that beam-column joints and beam end sections of traditional frame undergo a significant level of damage. Conversely, RC frame endowed with friction devices provide structural performance consistent with design forecasts, i.e. beam end sections with a nearly-elastic behaviour, panel zones which experience negligible level of damage, similar values of both maximum interstorey drift ratio and amount of energy dissipated with respect to traditional frame.

ACKNOWLEDGEMENTS

The economic support to the research of the SICILFERRO TORRENOVESE s.r.l. company is acknowledged, and the Authors thank Dr. Mauro Scurria and Eng. Nicolò Cancelliere for helpful discussion and active participation in the research project.

REFERENCES

- Borzouie, J., G. A. Macrae, J. G. Chase, G. W. Rodgers, and G. C. Clifton. 2016. Experimental Studies on Cyclic Performance of Column Base Strong Axis-Aligned Asymmetric Friction Connections. *Journal of Structural Engineering (United States)*, 142(1).
- Butterworth, J.W., Clifton, C.G., 2000. Performance of hierarchical friction dissipating joints in moment resisting steel frames, *Proc. of "12th World Conference on Earthquake Engineering"*, 30 January - 4 February, Auckland, New Zealand.
- Colajanni, P., La Mendola, L., Latour, M., Monaco, A., Rizzano, G., 2015. FEM Analysis of Push-out Test Response of Hybrid Steel Trussed Concrete Beams (HSTCBs), *Journal of Constructional Steel Research*, **111**, 88-102.
- Colajanni, P., La Mendola, L., Monaco, A., Spinella, N., 2016. Cyclic behavior of composite truss beam-to-RC column joints in MRFs, *Key Engineering Materials*, **711**, 681-689.
- Colajanni, P., La Mendola, L., Monaco, A., 2018a. Review of Push-out and Shear Response of Hybrid Steel-Trussed Concrete Beams, *Buildings*, **8**(10), art. n. 134.
- Colajanni, P., La Mendola, L., Monaco, A., 2018b. Stress Transfer and Failure Mechanisms in Steel-Concrete Trussed Beams: Experimental Investigation on Slab-Thick and Full-Thick Beams. *Construction and Building Materials*, **161**(1), 267-281.
- Colajanni, P., La Mendola, L., Monaco, A., Pagnotta, S., 2019. Design of friction connections in R.C. structures with hybrid steel-trussed-concrete beams, "XVII Convegno Anidis", 15-19 Settembre, Ascoli Piceno, Italia.
- Eligehausen, R., Popov, E.P., Bertero, V.V., 1983. Local bond stress-slip relationships of deformed bars under generalized excitations, *Report No. UCB/EERC-83/23*, College of Engineering, University of California, Berkeley, California.
- Khoo, H. H., C. Clifton, G. Macrae, H. Zhou, and S. Ramhormozian. 2015. Proposed Design Models for the Asymmetric Friction Connection. *Earthquake Engineering and Structural Dynamics* **44**(8),1309–24.
- Latour, M., Piluso, V., Rizzano, G., 2015. Free from damage beam-to-column joints: Testing and design of DST connections with friction pads. *Engineering Structures*, **85**, 219–233.
- Latour, M., D'Aniello, M., Zimbru, M., Rizzano, G., Piluso, V., Landolfo, R., 2018. Removable friction dampers for low-damage steel beam-to-column joints, *Soil Dynamics and Earthquake Engineering*, **115**, 66-81.
- Latour, M., Rizzano, G., Santiago, A., Simões da Silva, L., 2019. Experimental response of a low-yielding, self-centering, rocking column base joint with friction dampers, *Soil Dynamics and Earthquake Engineering*, **116**, 580-592.
- Lowes, L.N., Altoontash, A., 2003. Modeling reinforced-concrete beam-column joints subjected to cyclic loading, *ASCE Journal of structural engineering*, **129**(12), 1686-1697.
- Morgen, B.G., Kurama, Y.C., 2004. A friction damper for post-tensioned precast concrete moment frames, *PCI Journal*, **49**(4), 112-133.
- Pan, Z., Guner, S., Vecchio, F.J., 2017. Modeling of interior beam-column joints for nonlinear analysis of reinforced concrete frames, *Engineering Structures*, **142**, 182-191. DOI: 10.1016/j.engstruct.2017.03.066.
- Ramhormozian, S., Clifton, C.G., MacRae, G.A., Khoo, H.H., 2018. The Sliding Hinge Joint; final steps towards an optimum low damage seismic-resistant steel system, *Key Engineering Materials*, **763**, 751-760.
- SeismoSoft. SeismoStruct – a computer program for static and dynamic nonlinear analysis of frames structures, 2016. Available at <http://www.seissoft.com>.
- Sivaselvan, M.V., Reinhorn, A.M., 1999. Hysteretic models for cyclic behavior of deteriorating inelastic structures, *Tech. Rep. MCEER-99-0018*, Multidisciplinary Ctr. for Earthquake Engrg. Res., State University of New York at Buffalo, Buffalo, N.Y.
- Sivaselvan, M.V., Reinhorn, A.M., 2000. Hysteretic models for deteriorating inelastic structures, *ASCE Journal of engineering mechanics*, **126**(6), 633-640.
- Stevens, N.J., Uzumeri, S.M., Collins, M.P., 1991.

- Reinforced-concrete subjected to reversed-cyclic shear – Experiments and constitutive model, *ACI Structural Journal*, **88**(2), 135-146.
- Tsampras, G., Sause, R., Fleischman, R.B., Restrepo, J.I., 2018, Experimental study of deformable connection consisting of friction device and rubber bearings to connect floor system to lateral force resisting system, *Earthquake Engineering & Structural Dynamics*, **47**(4), 1032-1053.
- Vecchio, F.J., Collins, M.P., 1986. The modified-compression field theory for reinforced-concrete elements subjected to shear, *ACI Journal*, **83**(2), 219-231.
- Yang, T.S. & Popov, E.P., 1995. Experimental and analytical studies of steel connections and energy dissipators, *Report No. UCB/EERC-95/13*, University of California, Berkeley.
- Zimbru, M., M. D’Aniello, A. De Martino, M. Latour, G. Rizzano, and V. Piluso. 2018. Investigation on Friction Features of Dissipative Lap Shear Connections by Means of Experimental and Numerical Tests. *Open Construction and Building Technology Journal* **12**,154–69.